Exp Brain Res (2008) 188:77–89
DOI 10.1007/s00221-008-1340-x

RESEARCH ARTICLE

Time-invariant reference frames for parietal reach activity

Christopher A. Buneo · Aaron P. Batista · Murray R. Jarvis · Richard A. Andersen

Received: 18 July 2007 / Accepted: 29 February 2008 / Published online: 27 March 2008

Abstract Neurophysiological studies suggest that the transformation of visual signals into arm movement commands does not involve a sequential recruitment of the various reach-related regions of the cerebral cortex but a largely simultaneous activation of these areas, which form a distributed and recurrent visuomotor network. However, little is known about how the reference frames used to encode reach-related variables in a given "node" of this network vary with the time taken to generate a behavioral response. Here we show that in an instructed delay reaching task, the reference frames used to encode target location in the parietal reach region (PRR) and area 5 of the posterior parietal cortex (PPC) do not evolve dynamically in time; rather the same spatial representation exists within each area from the time target-related information is first instantiated in the network until the moment of movement execution. As previously reported, target location was encoded predominantly in eye coordinates in PRR and in both eye and hand coordinates in area 5. Thus, the different computational stages of the visuomotor transformation for reaching appear to coexist simultaneously in the parietal cortex, which may facilitate the rapid adjustment of trajectories that are a hallmark of skilled reaching behavior.

Keywords Monkey · Cortex · Arm · Coordinates · Transformations

C. A. Buneo · A. P. Batista · M. R. Jarvis · R. A. Andersen
Division of Biology, California Institute of Technology,
Mail Code 216-76, Pasadena, CA 91125, USA

C. A. Buneo (✉)
Harrington Department of Bioengineering,
Arizona State University, P.O. Box 879709,
Tempe, AZ 85287-9709, USA
e-mail: cbuneo@asu.edu

Present Address:
A. P. Batista
Department of Bioengineering, University of Pittsburgh,
BST3 4074, 3501 Fifth Avenue, Pittsburgh, PA 15261, USA

Introduction

The parieto-frontal network (PFN) is a collection of reciprocally connected cortical fields that appear to play a critical role in the planning and execution of arm movements (Wise et al. 1997; Caminiti et al. 1998). The functional properties of neurons in this network have been studied extensively using variants of the instructed delay task, a behavioral paradigm that temporally dissociates activation related to visual stimulation, movement planning/preparation, and movement execution. Although PFN neurons can be found that respond only during distinct periods of an instructed delay trial, many neurons in the PFN respond to all phases of the task, that is, from the moment an instructional stimulus or "cue" is presented until the time of movement execution (Shen and Alexander 1997; Snyder et al. 1997; Batista et al. 1999; Battaglia-Mayer et al. 2000, 2001; Messier and Kalaska 2000; Buneo et al. 2002; Russo et al. 2002). Such findings have led to the conclusion that visuomotor transformations for reaching are enabled by a simultaneous, rather than serial, recruitment of the different subdivisions of the PFN (Burnod et al. 1999).

Although neurons in the PFN can exhibit visual, plan and motor-related activation, it is presently unclear whether these neurons encode reach-related variables in the same reference frame throughout the different phases of an instructed delay trial or whether different reference frames are used at different times. We have previously reported

that during the *memory* period of an instructed delay task, neurons in the parietal reach region (PRR) encode the location of previously viewed targets in an eye-centered frame of reference (Batista et al. 1999). We have also reported that during the *perimovement* and memory periods of the same task, area 5 neurons encode the location of memorized targets simultaneously in both eye and hand coordinates (Buneo et al. 2002). Here we report an analysis of the reference frames for target location in both areas as a function of time within a trial. This investigation revealed that at both the single cell and population levels, the reference frames for encoding location did not evolve dynamically within PRR and area 5 but were fixed as a function of time. These results suggest that, in general, the various stages of the coordinate transformation for reaching do not evolve gradually in time; rather, once target-related information is instantiated in the network, all stages of the transformation exist simultaneously. This scheme may allow areas involved in the planning and monitoring of visually guided reaches to exert influence over the execution process with the shortest possible delay, enabling a rapid updating of reach trajectories in response to perturbations of either the goal or moving limb.

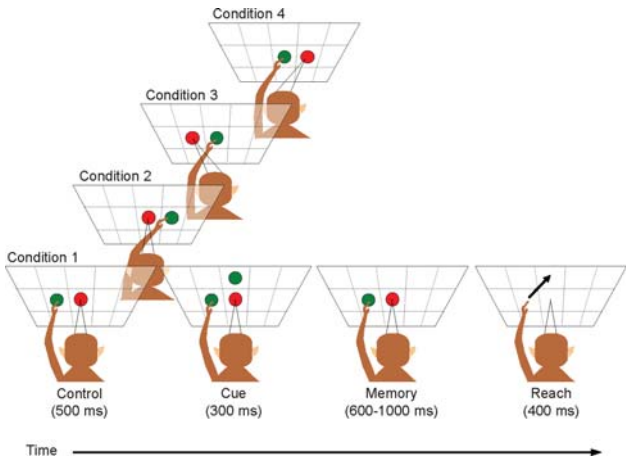

Fig. 1 Behavioral Paradigm. Neurons were studied using four randomly interleaved experimental conditions. The complete sequence of behavioral events was the same for all conditions but is illustrated here only for Condition 1. After the initial hand and fixation positions were acquired and maintained for 500 ms ("Control"), a reach target was briefly presented at another random board location ("cue" duration: 300 ms). Following the offset of this cue, a variable duration "memory" period ensued (range 600–1,000 ms). At the conclusion of this memory period, the LEDs signaling the initial hand and fixation positions were turned off and the animal reached to the remembered location of the target in complete darkness while maintaining fixation. Reach duration was variable but analysis of the perimovement period was restricted to a fixed 400 ms epoch centered on movement onset (200 ms before to 200 ms after)

Methods

Behavioral paradigm and neurophysiology

The behavioral paradigm and neurophysiological methods have been discussed in detail elsewhere (Batista et al. 1999; Buneo et al. 2002, 2003). In brief, neurons were studied in an instructed delay-reaching task that consisted of four randomly interleaved experimental conditions (Fig. 1). In two conditions, gaze was held fixed at the center position of the board and initial hand location was varied to the left (Condition 1) or right (Condition 2) of this center position. In the other two conditions, initial hand location was located at the center position and gaze was varied either to the left (Condition 3) or to the right (Condition 4) of center. For each condition, reaches were typically made between 8 and 11 buttons located immediately surrounding the initial hand position and/or within an adjacent column of buttons.

All experimental procedures were conducted according to the "Principles of laboratory animal care" (NIH publication no. 86-23, revised 1985) and were approved by the California Institute of Technology Institutional Animal Care and Use Committee. Single cell recordings were obtained from the right hemispheres of two adult rhesus monkeys (*Macaca mulatta*) using standard neurophysiological techniques. Recordings were made in both the parietal reach region (PRR), which overlaps the medial intraparietal area (MIP) and area V6A (Snyder et al. 1997), and area 5 of the PPC. The PRR data described in this study ($N = 87$, 23 from animal CKY and 65 from animal DNT) consist of all neurons from animals CKY and DNT that were included in Batista et al. (1999) plus some additional neurons recorded afterward. The area 5 data discussed here ($N = 89$, 61 from animal CKY and 28 from animal DNT) were obtained during the same experimental sessions as those reported in Buneo et al (2002).

Data analysis

Peristimulus time histograms (PSTHs) of the mean firing rate of single neurons were constructed for each target location by smoothing the spike train with a Gaussian kernel ($\sigma = 50$ ms). Confidence intervals were estimated from a distribution of PSTHs obtained by bootstrapping over trials (Efron and Tibshirani 1993).

Reference frames

To plan a reaching movement, the brain must compute the difference between target location (*T*) and the initial or current hand location (*H*), that is, the desired movement vector. Since the movement vector is defined by the location of the target relative to the hand, we will also refer to

this vector as T_H, for "target location in hand-centered coordinates". Information about both T and H can in many instances be derived from vision, thus a desired movement vector can be computed by subtracting H from T in a visual or eye-centered (E) reference frame (Buneo et al. 2002), that is,

$$T_H = T_E - H_E \quad (1)$$

Alternatively, T and H can be encoded in body-centered (B) coordinates (Flanders et al. 1992; Henriques et al. 1998; McIntyre et al. 1998), thus, the movement vector could be computed as

$$T_H = T_B - H_B \quad (2)$$

Although either scheme (or both) could conceivably be used by the motor system, we sought to identify the experimental variable or combination of variables (i.e., T_E, H_E, T_B, H_B, etc.), which best accounted for the responses of parietal neurons during memory-guided reaching. We reasoned that if H and/or T are encoded in a particular frame (such as eye coordinates) then neural activity should not vary if H and T are held constant in that frame, but varied in other frames (such as body or world coordinates). Thus, the combination of variables that "best-fit" the responses of parietal neurons would be those variables that were associated with the least amount of variability in neural activity. To test this, we quantified the invariability of parietal activity when T or both T and H were held fixed within a particular reference frame, and all the remaining experimental variables were allowed to vary. The following five combinations of variables were examined: (A) same T in hand coordinates (i.e., same movement vector), (B) same T in body coordinates, (C) same T in eye coordinates, (D) same T and H in body coordinates, and (E) same T and H in eye coordinates. For A, B, C, and E, gaze position and the initial hand position on the board varied by one position each, while for D, gaze varied by two positions and initial hand position on the board was fixed (see Fig. 5). Thus, the net variation in gaze and initial hand position was the same for all 5 comparisons (net variation = 2).

For each combination of variables, we paired the mean firing rates for a given reach in one condition with all corresponding reaches from the other task conditions. The results of this pairing procedure can be seen in Fig. 5. Each panel of this figure shows the mean firing rate for five repetitions of a given movement, for example, up and to the left or down and to the right, plotted against the response for five repetitions of the same movement from a different task condition. For each neuron, responses for all possible pairs of movements are plotted once. Due to the experimental design, however, the number of reach pairs that could be compared varied for the different combinations of variables. For example, for the same T in body coordinates (Fig. 5b), all four task conditions could and were used to produce the relevant pairings, while for the same T and H in body coordinates (Fig. 5d), only data from Conditions 3 and 4 could be used. As a result, the number of pairings that were analyzed (reflected by the number of data points in each panel of Fig. 5) varied for the different comparisons. The following numbers of data points were analyzed for each combination of variables in area 5: A: 2555, B: 1045, C: 928, D: 615, and, E: 1106. In PRR, these numbers were as follows: A: 2534, B: 1040, C: 951, D: 635, and E: 1110. These numbers correspond to the number of cells in each area multiplied by the number of possible reach pairings/cell.

The pairing procedure described above resulted in two vectors of firing rates for any given combination of variables. The invariability of these paired firing rates was initially estimated using the simple (or Pearson product-moment) correlation coefficient (Zar 1996). At the population level however, activity was generally well correlated in all reference frames, due in part to intrinsic differences in baseline firing rates among neurons, which "build-in" a degree of correlation. In fact, when all experimental variables (T, H, and gaze direction) were randomly varied, the correlations in both PRR and area 5 were still moderately strong ($r = \sim 0.6$). Thus, we also quantified invariability using a measure that is relatively insensitive to absolute firing rate. More specifically, invariability (INV) was quantified as:

$$\mathrm{INV} = \left(\sum_{i=1}^{n} (x_i - y_i)^2/2\right) \Big/ \left(\sum_{i=1}^{n} x_i^2 + y_i^2\right) \quad (3)$$

where x_i represents the mean firing rate of one neuron for a particular reach in one task condition and y_i represents the firing rate for a corresponding reach in a different condition. Thus the sums in the numerator and denominator are over all possible reach pairs (n). In Eq. 3, the numerator is equivalent to the sum of the squared distances to the unity line of all the data points in a given panel in Fig. 5, and the denominator is equivalent to the sum of the squared distances of these points to the origin. In terms of the meaning of specific values of INV, a value of 0 would be obtained if the data were perfectly correlated, that is, if $x_i = y_i$ for all i. A value of 1/8 (0.125) would be obtained if x and y were drawn from uniform random variables ranging from 0 to some maximum value.

In addition to estimating invariability for combinations of T and/or H in body and eye coordinates, for comparative purposes we also computed the invariability when the experimental variables were randomly shuffled such that x_i and y_i corresponded to different movements, gaze directions and initial hand positions (which provides an indication of the worst possible correlation). Lastly, we computed an estimate of the best correlation possible given

the trial-to-trial variability in the data. This estimate was obtained by correlating the activity for a given set of experimental variables with multiple, bootstrap resampled versions of the same data.

For both the correlation coefficient and INV, 95% confidence intervals were constructed by bootstrapping over trials (for individual cells) or over cells (for the population)(Efron and Tibshirani 1993). Statistical bootstrapping was also used to aid in the determination of statistically significant differences among the invariability values obtained for the different combinations of experimental variables. Using the correlation coefficients obtained for the population data as an example (Fig. 5), a distribution of such coefficients was obtained for each of the five combinations of variables by bootstrapping (i.e., resampling with replacement) the various cells in the population. Bootstrapping was performed 200 times for each combination of variables and the resulting distributions of correlation coefficients (one for each combination of variables) were then subjected to a Kruskal–Wallis test, equivalent to a one-way "analysis of variance by ranks" (Zar 1996). As would be the case with a parametric ANOVA, the non-parametric Kruskal–Wallis test required post hoc multiple comparisons to determine precisely where differences were located among the different distributions. In the present study, multiple comparisons based on Tukey's honestly significant difference criterion were used (Matlab, The Mathworks, Natick, MA). These multiple comparisons were used to identify the "best-fitting" combination of variables, that is, the best correlated grouping that was significantly different from all other combinations of variables. The same procedures were used to identify the best-fitting combination of variables for single cells, with the exception that 95% confidence intervals were constructed by bootstrapping over trials rather than over cells.

Temporal analysis

At both the single cell and population levels, invariability in all reference frames was quantified (using both the correlation coefficient and INV) during discrete behavioral epochs: a "cue" epoch lasting from 100–400 ms after the onset of the instructional (cue) stimulus, a "memory" epoch lasting from 400–800 ms after stimulus onset, and a perimovement or "reach" epoch lasting from 200 ms before until 200 ms after movement onset (defined as the time at which the animal released the button at the starting position). At the population level, invariability was also quantified using a sliding 200 ms long window centered on consecutive 100 ms intervals of the task. This latter analysis was performed using data aligned at both cue onset and movement onset (see Fig. 6).

For the single cells, we examined the temporal evolution of reference frames by considering whether the best-fitting combination of variables changed from the cue to the reach epoch. Only neurons that had a single, best-fitting combination of variables in all behavioral epochs were considered. For this analysis, cells were considered to be coding in eye coordinates if their activity varied least for either the same targets or for a given combination of targets and hand positions in eye coordinates, that is, the number of variables being encoded in this frame did not matter. Similarly, cells were considered body-centered if their responses varied least for the same targets or for a given combination of targets and hand positions in body coordinates.

Results

Figure 2 shows the responses of a single PRR neuron for Conditions 1–4. Each row in the figure corresponds to one condition. The first three panels show pseudocolor maps of the mean firing rate of the cell during the three discrete behavioral epochs defined in "Methods" (temporal analysis). In each map, mean firing rate is plotted as a function of board location, with the horizontal dimension of the reach board along the abscissa and the vertical dimension along the ordinate. This figure shows that the peak response of the cell, indicated by redder hues on the colormaps, is locked to the fixation point ("E"). For example, during the reach epoch (C), the location of the peak response of the cell did not vary for Conditions 1 and 2, despite the fact that movements to the same board location were achieved by different movements in these two conditions. However, when the eyes were fixated to the left (Condition 3) or right (Condition 4) of the center, the peak shifted in such a way that it was always in the same location with respect to the fixation point. This was true not only during the reach period but during the cue and memory periods as well (A, B). We interpret this pattern of activity as evidence that the cell encodes target location in an eye or fixation-centered frame of reference, in a manner that appears to be invariant with respect to time.

Panels D and E of Fig. 2 show PSTHs for reaches made to the lower middle location on the board (indicated by the highlighted area on the colormaps). As would be expected from the colormaps, activity was highest when the target appeared at the preferred location of the cell in eye coordinates (Conditions 3 and 4). Note also the very strong activation of the cell at cue onset (D) that is maintained throughout the early part of the movement (E). This is a common feature of PRR neurons (Snyder et al. 2000; Buneo et al. 2003), and reflects a strong influence of visually triggered instructional cues on cell activity in this area.

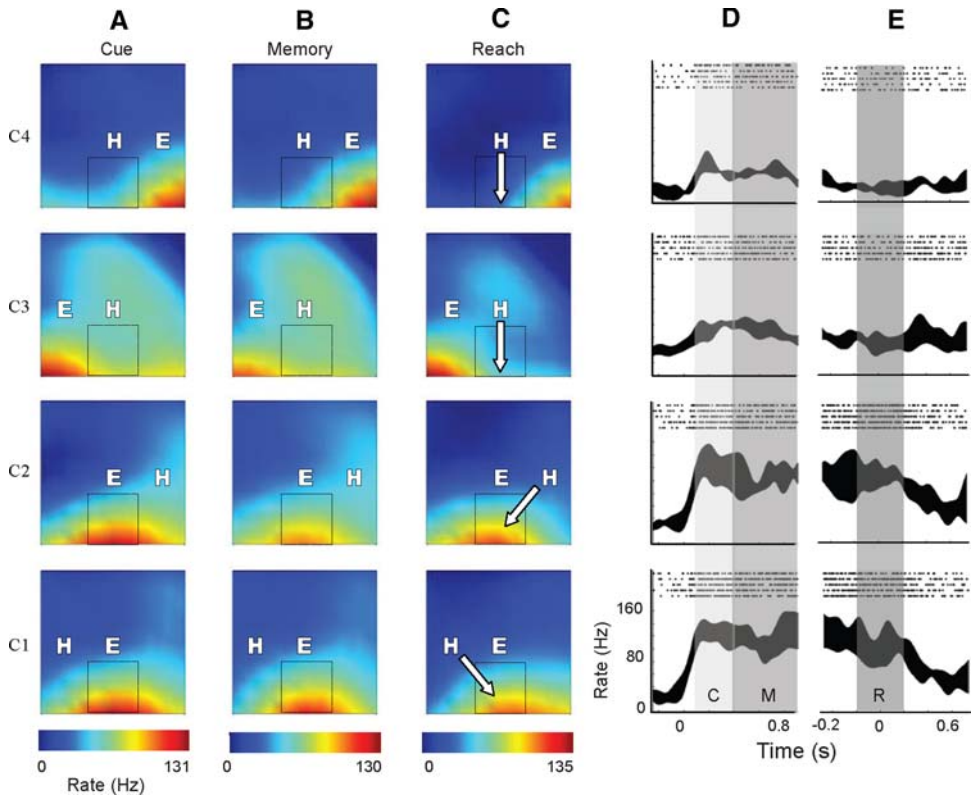

Fig. 2 A PRR neuron that encodes target position in eye-centered coordinates during all phases of an instructed delay task. **a–c** Colormaps of the mean firing rate of a PRR neuron for each task condition (C1–C4) during the cue, memory and reach periods, respectively. *Scale bars* differ across panels, but are the same for each row of a given panel. In each colormap, mean firing rate is plotted as a function of horizontal (*x* axis) and vertical (*y* axis) board position. Redder hues correspond to higher firing rates. Note that no activity is possible at the location in the colormaps corresponding to "*H*", which indicates the initial hand position, but is possible at "*E*", which indicates the fixation point. **d–e** PSTHs of the cell's mean firing rate for reaches to the lower middle board location, indicated by the *square* on the colormaps. Data are aligned to cue onset in **d** and to movement onset in **e**

Figure 3 shows another pattern of responses commonly observed in PRR. As with the previous cell, this neuron had a peak response that was locked to the fixation point; in this case the peak was always directly above where the animal was fixating. However, this cell exhibited a large difference in overall responsiveness for the different conditions. The firing rate of the cell was much greater in Conditions 2 and 3 than in Conditions 1 and 4. In many cells, this preference for particular groupings of the task conditions was even observed during the control period, indicating that this preference was related to the relative configuration of the eyes and hand, that is, the initial conditions, rather than to any difference in the movements themselves, which were not cued until later in the trial. Conditions 2 and 3 corresponded to initial conditions where the hand was to the right of the fixation point while Conditions 1 and 4 corresponded to initial conditions in which the hand was to the left of the fixation point. In other words, in Conditions 2 and 3 reaches were made from an identical starting position in eye coordinates (18° to the right), while in Conditions 1 and 4 the starting position was also identical in eye coordinates (18° to the left). If one compares the activity of the cell in Conditions 2 and 3 for the same targets in eye coordinates, the response of the cell appears largely identical (see Fig. 5e). This is also true for Conditions 1 and 4. Thus, the responses of this cell were most consistent for combinations of initial hand and target location in eye coordinates. As with the cell shown in Fig. 2, this trend was observed during all phases of the task (cue, memory and reach).

In contrast to the cells shown in Figs. 2 and 3, Fig. 4 shows a neuron from area 5 that appears to encode reach variables using a combination of eye and hand coordinates. As with the PRR neuron shown in Fig. 3, there is a large difference in overall firing rate among the four experimental conditions; the cell was much more active in Conditions 1 and 4, for example, than in Conditions 2 and 3. However the cell differs from the previous examples in one very important way: the tuning of the cell is not invariant with respect to the initial hand position, fixation point, or the board. In fact the response of this cell can only be accounted for if both the target location (in eye

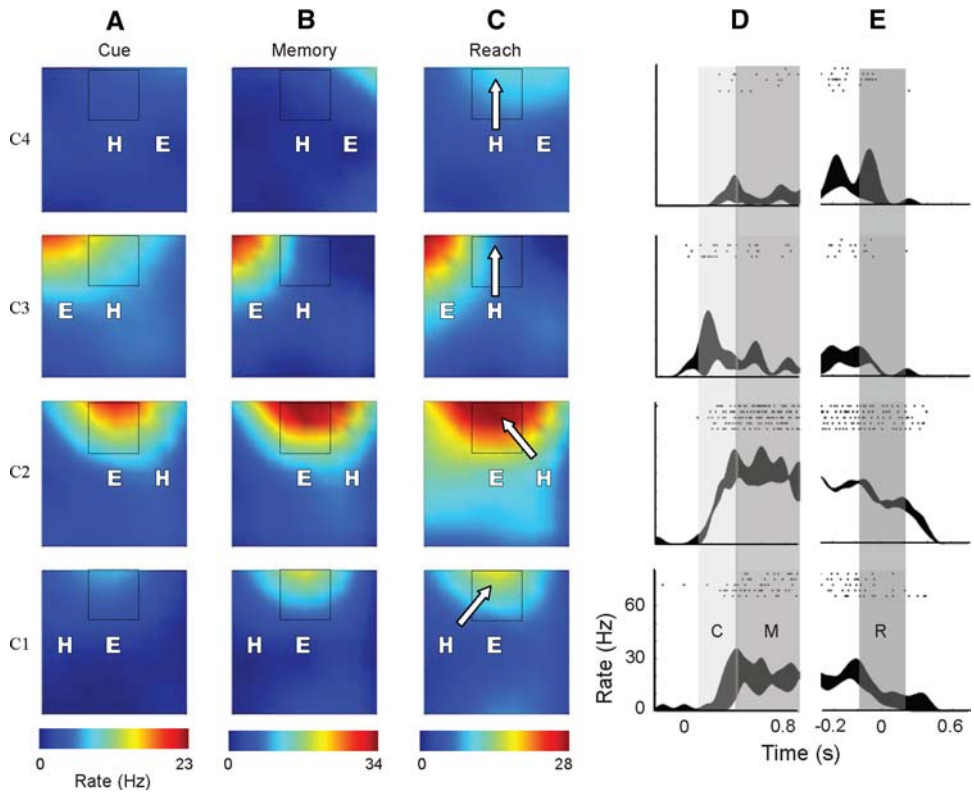

Fig. 3 A PRR neuron that appears to encode target position and initial hand position in eye coordinates. Figure conventions as in Fig. 2

coordinates) and planned movement vector are both taken into account (Buneo et al. 2002). This argues against a strictly eye, hand, or body-centered encoding scheme. Instead, the responses of this cell and many others in area 5 are consistent with an encoding of reach variables in both eye and hand coordinates, a point that will be reiterated later.

Panels D and E of Fig. 4 show PSTHs from the same cell for reaches made to the lower middle location on the board. As would be expected from the colormaps, activity for this board location was most similar when the relative configuration of the hand and eye were the same (i.e. Conditions 1 and 4, as well as Conditions 2 and 3). Note also the variation in firing rate as a function of time for this neuron. In contrast to both PRR neurons (Figs. 2, 3), activity at cue onset is relatively weak (D), and builds up during the task, peaking at or slightly after movement onset (E). This is a common feature of many area 5 neurons (Kalaska and Crammond 1995; Buneo et al. 2003), and may indicate that area 5 is more closely tied to the specification of motor output than PRR.

At the population level, activity in both area 5 and PRR was least variable for combinations of targets and initial hand locations in eye coordinates (Fig. 5). In each panel in Fig. 5, individual data points correspond to the mean firing rate of a single cell for two movements involving the same target in hand coordinates (A), same target in body coordinates (B), same target in eye coordinates (C), same target and initial hand location in body coordinates (D) and same target and initial hand location in eye coordinates (E). Data from all cells and all possible targets during the perimovement ("Reach") epoch are shown (see Table 1 for values of r and INV for other epochs). The scatter in each plot illustrates how well that particular coordinate frame or frames accounted for population activity in a given area. A low degree of scatter (i.e., a high degree of correlation) indicates a good fit to that combination of variables and reference frame, while a high degree of scatter (low correlation) indicates a poor fit. For example, Fig. 5a tests the hypothesis that PRR and area 5 encode the hand-centered movement vector, regardless of where the movement starts and ends with respect to the world, body or current gaze direction. Although activity in PRR and area 5 was reasonably well correlated for the same movement vectors (0.59 and 0.84, respectively), only the area 5 coefficient differed substantially from the correlation that was obtained when all experimental variables are randomly varied ($r = 0.6$). Activity in both areas was better correlated in Fig. 5e, which tests the hypothesis that cell activity encodes a movement vector defined by a particular starting location and target location with respect to gaze (i.e., in eye coordinates). Statistical analyses of the data in Fig. 5 confirmed that area 5 and PRR population activity were best correlated for combinations of targets and initial hand locations in eye coordinates (Kruskal–Wallis test with nonparametric multiple comparisons ($P < 0.05$)).

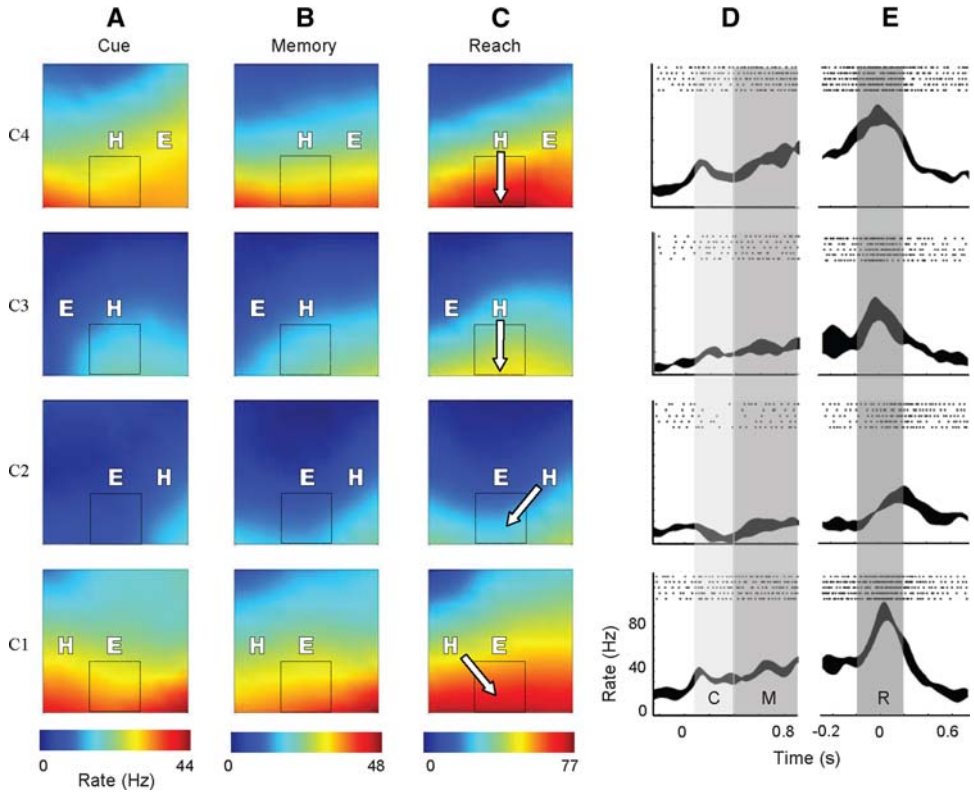

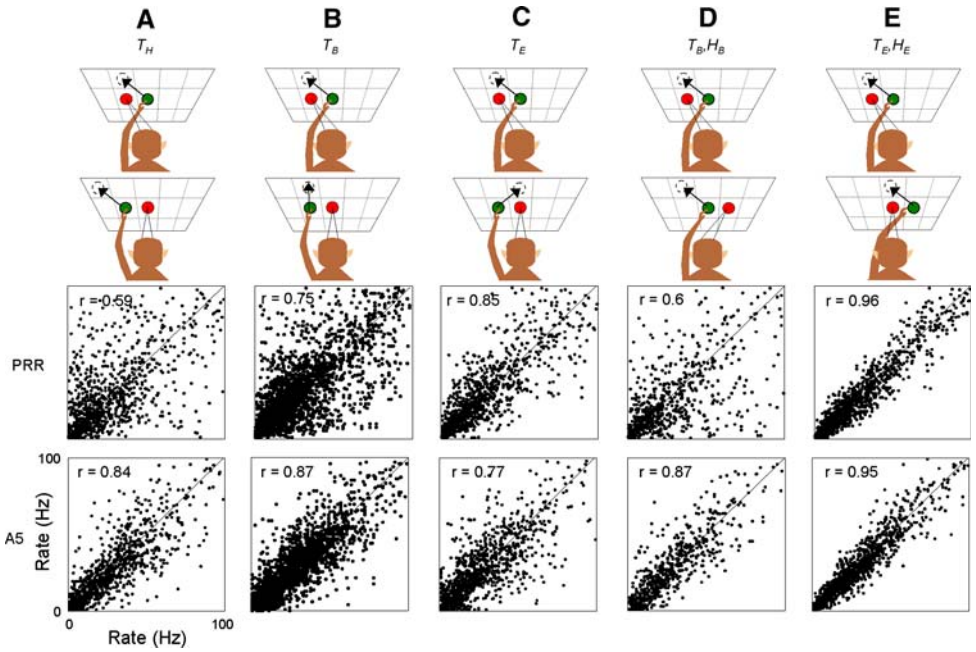

Fig. 4 An area 5 neuron that appears to encode target position in both eye and hand coordinates. Figure conventions as in Fig. 2

Fig. 5 PRR and area 5 population activity during the reach epoch. Each data point corresponds to one cell's firing rate for a pair of movements; movements in a pair were taken from different experimental conditions and were randomly assigned to the ordinate or abscissa. Movements in a pair were associated with **a** identical targets in hand coordinates (T_H), **b** targets in body coordinates (T_B), **c** targets in eye coordinates (T_E), **d** targets and initial hand locations in body coordinates (T_B, H_B), and **e** targets and initial hand locations in eye coordinates (T_E, H_E). To aid visual comparison, all plots were truncated at 100 Hz, though data from all cells and all possible pairings were used to calculate the corresponding correlation coefficients

Table 1 Correlation coefficients and INV values for each area, animal and epoch

		TH	TB	TE	TB, HB	TE, HE	Shuffled
Area 5 "reach" epoch							
CKY	*r*	0.7876	0.8611	0.7414	0.8504	0.9498	0.6836
	INV	0.0386	0.0249	0.0453	0.0273	0.0090	0.0565
DNT	*r*	0.8842	0.8810	0.8042	0.8953	0.9502	0.7064
	INV	0.0288	0.0285	0.0446	0.0260	0.0116	0.0679
Both	*r*	0.8372	0.8716	0.7731	0.8737	0.9502	0.6974
	INV	0.0343	0.0264	0.0455	0.0267	0.0101	0.0589
"Memory" epoch							
CKY	*r*	0.7045	0.7959	0.6769	0.7729	0.9143	0.5224
	INV	0.0544	0.0366	0.0573	0.0456	0.0154	0.0873
DNT	*r*	0.8284	0.8405	0.7428	0.8532	0.9514	0.658
	INV	0.0557	0.0521	0.0823	0.0494	0.0164	0.1088
Both	*r*	0.7636	0.8138	0.7100	0.8004	0.9311	0.5689
	INV	0.0549	0.0421	0.0660	0.0470	0.0158	0.0965
"Cue" epoch							
CKY	*r*	0.6737	0.7663	0.6257	0.7355	0.9091	0.4806
	INV	0.0603	0.0425	0.0677	0.0511	0.0168	0.0899
DNT	*r*	0.8995	0.8656	0.7288	0.8990	0.9414	0.6641
	INV	0.0335	0.0444	0.0858	0.0331	0.0194	0.1254
Both	*r*	0.7797	0.8156	0.6774	0.8124	0.9237	0.5923
	INV	0.0515	0.0431	0.0737	0.0448	0.0177	0.0969
PRR "reach" epoch							
CKY	*r*	0.8876	0.9286	0.9185	0.9176	0.9600	0.8118
	INV	0.0246	0.0160	0.0181	0.0174	0.0094	0.0375
DNT	*r*	0.4955	0.6836	0.8244	0.4913	0.9475	0.4664
	INV	0.1121	0.0692	0.0380	0.1141	0.0117	0.118
Both	*r*	0.5946	0.7485	0.8486	0.5974	0.9504	0.5585
	INV	0.0882	0.0543	0.0327	0.0879	0.0111	0.0932
"Memory" epoch							
CKY	*r*	0.7648	0.8919	0.9012	0.8386	0.9372	0.6086
	INV	0.0450	0.0206	0.0187	0.0372	0.0120	0.063
DNT	*r*	0.3865	0.6149	0.8192	0.4148	0.9151	0.3082
	INV	0.1274	0.0818	0.0403	0.1264	0.0195	0.1468
Both	*r*	0.5227	0.7059	0.8441	0.5291	0.9214	0.4447
	INV	0.0988	0.0613	0.0988	0.0987	0.0170	0.1215
"Cue" epoch							
CKY	*r*	0.7496	0.8762	0.9013	0.8617	0.9544	0.5795
	INV	0.0499	0.0248	0.0197	0.0348	0.0091	0.0808
DNT	*r*	0.5172	0.6873	0.8298	0.5320	0.9304	0.2589
	INV	0.0999	0.0642	0.0356	0.0980	0.0149	0.1496
Both	*r*	0.5831	0.7387	0.8480	0.6015	0.9369	0.377
	INV	0.0855	0.0532	0.0314	0.0811	0.0132	0.1296

The basic trend illustrated in Fig. 5 was observed not only during the perimovement period but also throughout the entire task. Figure 6 shows the invariability measure defined in Eq 3 plotted as a function of time. In this figure, the INVs for different combinations of variables have been normalized to the value of INV obtained when the experimental variables where randomly shuffled (see "Methods"). In other words, INVs have been normalized by an estimate of the maximum variability possible in this experiment. Five different curves are shown, corresponding to the five combinations of reach-related variables described in "Methods" and illustrated graphically in Fig. 5.

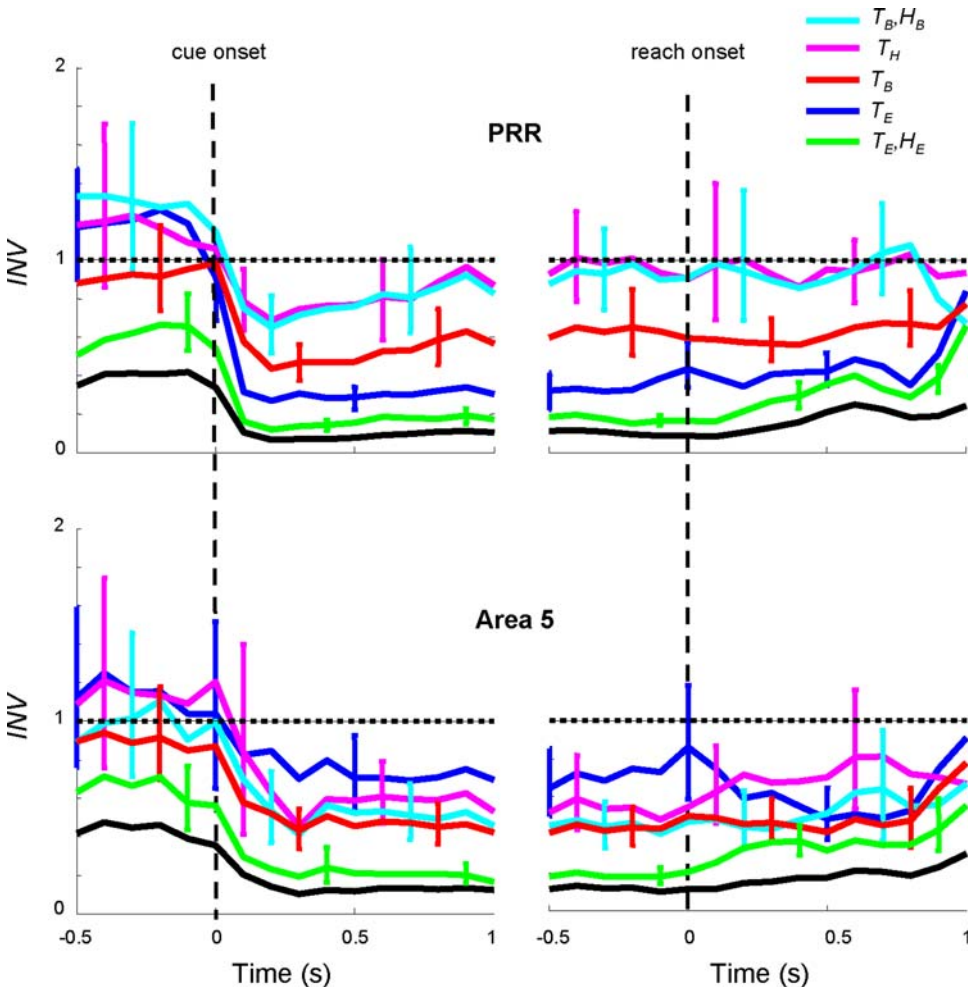

Fig. 6 Invariability (INV) of PRR (*top*) and area 5 (*bottom*) population activity [normalized by an estimate of the maximum possible variability (*dotted black line* at INV = 1)] for different combinations of reach variables and reference frames, as a function of time. Data aligned on both cue onset (*left*) and movement onset (*right*) are shown. For clarity, *error bars* (representing the 95% confidence intervals obtained via statistical bootstrapping) are shown in 500 ms intervals. The *solid black curve* is an estimate of the least possible variability, given the trial-to-trial variability in the data (see "Methods" for details)

Smaller values of INV correspond to lower degrees of scatter. At cue onset, activity in both the areas became less variable in all reference frames, indicating that target location was encoded in both areas. However, activity in PRR and area 5 tended to be least variable for combinations of targets and initial hand locations in eye coordinates (green curve), and was nearly as invariable as it could be, given the trial-to-trial variability in the data (black curve). This tendency persisted throughout the delay period and the initial phases of the movement. Interestingly, this trend was also observed during the control period, that is, prior to cue onset. At this point in the trial there was no information about the target location, thus the lower degree of scatter during this epoch can only be attributed to a substantial number of neurons encoding initial hand location in eye coordinates.

As the icons above Fig. 5e show, a given combination of hand position and target position in eye coordinates corresponds to a unique hand-centered movement vector. Thus, the invariability of parietal activity for combinations of targets and hand positions in eye coordinates could conceivably be due to the fact that neurons are encoding reach variables only in eye coordinates or using a combination of eye and hand coordinates. In fact, both types of neurons can be found in the parietal cortex: PRR neurons appear to encode reach-related variables predominantly in eye coordinates, while area 5 neurons encode these variables in both eye and hand coordinates. Two lines of evidence support this conclusion. First, as pointed out earlier, when data were analyzed for the same targets in hand coordinates in PRR (e.g., Fig. 5a), the resulting correlation coefficient ($r = 0.59$) did not differ substantially from the correlation that was obtained when all experimental variables are randomly varied ($r = 0.6$). This suggests that an encoding of target position in hand coordinates does not contribute to the low degree of scatter observed for PRR in Fig. 5e. In contrast, the correlation obtained for the same targets in hand coordinates in area 5 ($r = 0.84$) was substantially greater than that obtained when all experimental variables were randomized (also approximately 0.6 in this area). The correlation in area 5 was still greater, however, when movement vectors were associated with a particular target and hand location in eye coordinates. These observations suggest that the low

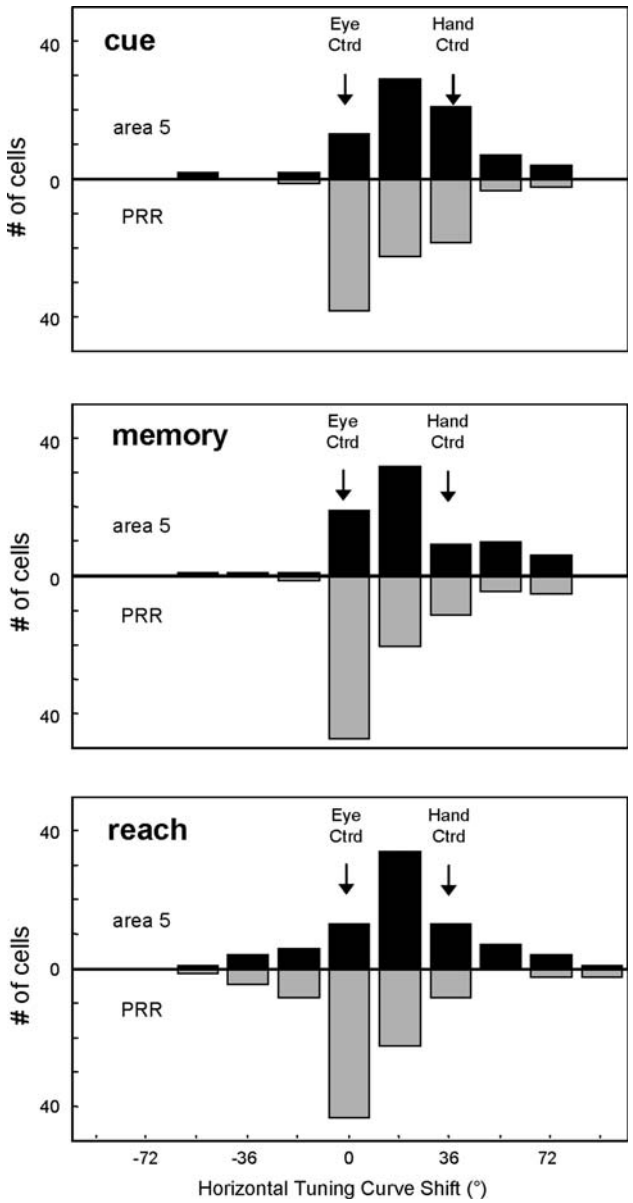

Fig. 7 Distribution of horizontal tuning curve "shifts" (in degrees of visual angle) for area 5 and PRR when initial hand location was varied from left to right by 36° (in eye coordinates). Data for the cue, memory and reach epochs are shown

degree of scatter in Fig. 5e for area 5 arises from an encoding in both eye and hand coordinates, though they do not indicate whether this arises from two distinct populations of neurons (one eye-centered, one hand-centered), or in part from a population of neurons that encodes in both frames simultaneously.

The second line of evidence supporting different spatial representations in PRR and area 5 comes from a population analysis of tuning curve shifts. As illustrated previously (Buneo et al. 2002), if targets are encoded purely in eye coordinates, tuning curves for target location should not shift when initial hand location is varied, while if they are encoded in both eye and hand coordinates these tuning curves should appear to partially shift with respect to one another, reflecting a compromise between the eye and hand reference frames. Figure 7 shows for both area 5 and PRR the distribution of tuning curve shifts when initial hand location was varied from left to right by 36°. Due to the experimental design, shifts could only be classified as multiples of the spacing between reach targets, which was 18° of visual angle. For the cue, memory and reach epochs, the largest percentage of area 5 neurons exhibited a tuning curve shift of 18°, that is, a partial shift, consistent with an encoding of target location in both eye and hand coordinates. Figure 7 also shows the same analysis applied to the PRR data. For the cue, memory, and reach epochs, the largest percentage of cells showed a tuning curve shift of 0°, consistent with a purely eye-centered coding of target location. Thus, not only are the spatial representations different in PRR and area 5 but within each area these representations appear to be invariant with respect to time.

Although our analysis of population activity in PRR and area 5 points to time invariant spatial representations for the encoding of reach-related variables, it is still possible that individual neurons in these areas exhibited a dynamic evolution of their "best-fitting" combination of reach variables (and corresponding reference frame) with time. For example, it is possible that some neurons were coding target location in eye coordinates during the cue period, but in hand or body-centered coordinates as movement onset approached. Such a neuron would in effect be mimicking, on a very slow time scale, the inverse kinematic transformations required to place the hand on the target; thus we will refer to this putative cell type as a "pseudo inverse" neuron. It is also possible that some neurons showed the reverse trend, that is, encoding in hand or body coordinates at the cue and later in eye coordinates. This type of neuron, if it existed in significant numbers, could provide evidence that an area plays a role in transforming motor-related signals into a prediction of the position of the hand, in eye coordinates, after a planned movement is completed. As this computation would require access to a forward model, we will refer to this putative cell type as a "pseudo forward" neuron.

In order to examine this question, we estimated the invariability of single neuron activity when reach-related variables were held fixed in eye, hand and/or body coordinates. Although we used the same measure of invariability that was used for the population data, for simplicity we confined our single cell analysis to the discrete behavioral epochs described earlier (cue, memory, reach), rather than the more "continuous" time bins shown in Fig. 6. We first identified the "best-fitting" combination of reach variables and reference frame for each neuron in each epoch. In PRR, 65/89 cells (73%), 62/89 (70%), and

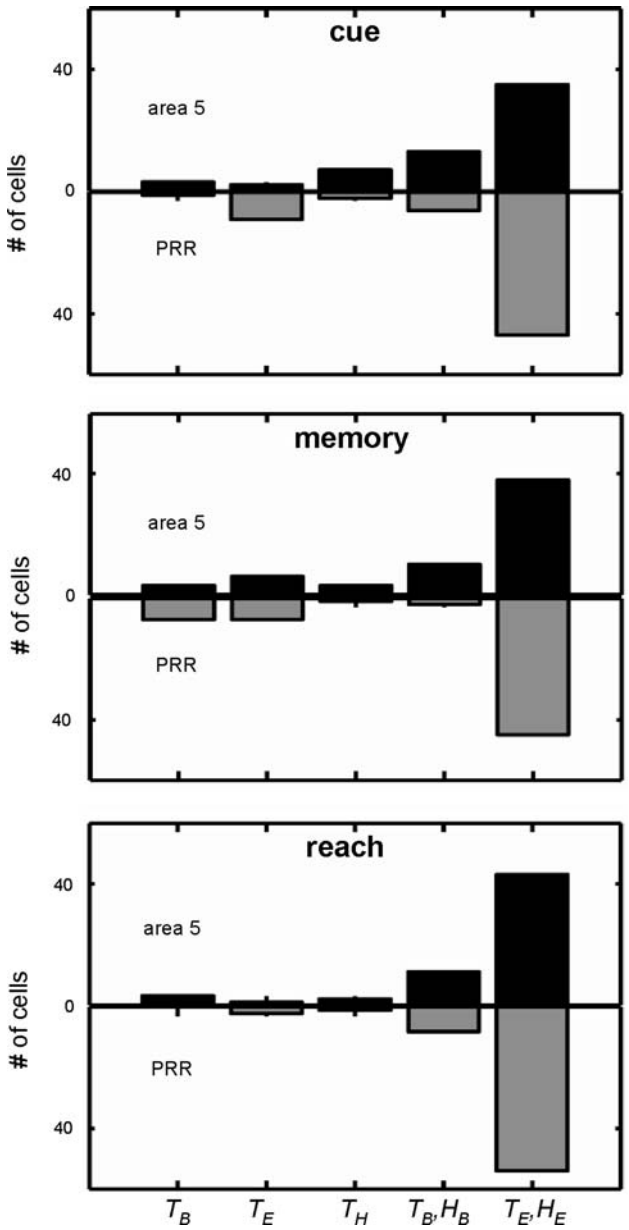

Fig. 8 Preferred combinations of reach variables/reference frames for individual neurons. Shown for each epoch are the number of neurons in each area that showed the least variation in their firing rate for identical targets in body coordinates (T_B), targets in eye coordinates (T_E), targets in hand coordinates (T_H), targets and initial hand locations in body coordinates (T_B, H_B), or targets and initial hand locations in eye coordinates (T_E, H_E)

65/89 (73%), had a single, best fitting combination of variables in the cue, memory and reach epochs, respectively [Kruskal–Wallis test with non-parametric multiple comparisons ($P < 0.05$)]. Similarly in area, 5, 60/87 neurons (69%) had a single best-fitting combination of variables in each epoch. The number of neurons showing a preference for each combination of variables is shown in Fig. 8; this figure shows that in both area 5 and PRR the dominant combination of variables in any given epoch was targets and initial hand locations in eye coordinates (T_E, H_E), in agreement with the population analysis described earlier.

The results described in the previous paragraph do not exclude the possibility that some neurons switched their best fitting reference frame from the cue to the reach epoch, and vice-versa. Thus, we next determined the percentage of cells in each area that could be classified as "pseudo inverse", that is, those that changed their best fitting frame from eye to hand or body coordinates as a trial progressed, or "pseudo forward", those that changed from hand or body to eye coordinates. For this analysis we considered only those neurons that had a single, best-fitting combination of variables in all behavioral epochs; this criterion reduced our dataset to 38 neurons in PRR and 32 neurons in area 5. Since the best-fitting combination of variables during the memory period was generally the same as either the cue or reach period, we report only how these variables differed between the cue and reach periods. The results of the analysis were as follows: 35/38 PRR neurons (92%) and 24/32 area 5 neurons (75%) showed the least variability for the *same* combination of reach variables in both the cue and reach epochs, that is, the majority of our subset of PRR and area 5 neurons showed no evidence of a temporally evolving reference frame. As a result, few neurons in either area could be classified as "pseudo inverse" or "pseudo forward". In PRR, 2/38 or 5% of the neurons were classified as "pseudo inverse" while no neurons were classified as "pseudo forward". In area 5, 4/32 (12.5%) of the neurons were classified as "pseudo inverse" and 3/32 (9%) were classified as "pseudo forward". Thus, for the populations as a whole, only 2/89 PRR neurons (2%) and 7/87 area 5 neurons (8%) could be definitively described as being either inverse or forward transform cells, providing further support for the idea that spatial representations in the parietal reach areas are generally static with regard to reference frames.

Discussion

We report here an analysis of the reference frames in area 5 and PRR of the PPC as a function of time in an instructed delay-reaching task. Our analysis revealed that, at both the single cell and population levels, the reference frames for encoding target location did not evolve dynamically within each area but were fixed as a function of time. As previously reported, this frame was predominantly fixed to the eyes in PRR (Batista et al. 1999) and to both the eye and hand in area 5 (Buneo et al. 2002). These results suggest that the various stages of the coordinate transformation for reaching do not evolve gradually in time within the PFN; rather, once

target-related information is instantiated in the network, all stages of the transformation exist simultaneously.

The finding of adjacent parietal regions encoding target locations relative to the eye (PRR) and to both the eye and hand (area 5) suggests that, at least in certain contexts, targets are transformed directly from eye to hand-centered coordinates in the PFN. The transformation is *direct* in the sense that it does not require targets to be transformed into intermediate head and body-centered representations. This should not be construed to mean that all the computations required to produce an appropriate motor command have been accounted for at this computational stage (Crawford et al. 2004). The hand-centered representation in area 5 could represent a desired movement vector. However, only an intrinsic, arm-centered representation, that is, one expressed in terms of changes in arm orientation, can be used as an input to structures concerned with specifying movement dynamics or patterns of muscle activation (Flanders et al. 2003). Thus, further computations either within or downstream of area 5 must transform the hand-centered movement vector into an appropriate intrinsic representation. Mechanistically, signals encoding eye, head and arm orientation, which are ubiquitous within the PFN, likely play an important role in this transformation (Buneo and Andersen 2006).

The present results are consistent with the predictions of neural network models of coordinate transformations (Zipser and Andersen 1988; Salinas and Abbott 1995; Xing and Andersen 2000; Deneve et al. 2001; Smith and Crawford 2001). Such models generally consist of an input layer that encodes incoming spatial information in one reference frame (e.g., eye coordinates), an output layer coding in another reference frame (e.g., head or body-centered coordinates), and one or more intermediate layers that serve to map the inputs to the outputs. Transformations between the reference frames are achieved by establishing, through training, a precise pattern of connectivity between the different layers of the network. Once this connectivity is established, however, each stage of the transformation (signified by the input, output and intermediate layers) can be thought to coexist simultaneously. Activation of the trained network results in an immediate, rather than serially evolving, transformation, a finding suggested by the present results as well. Moreover, intermediate layers of these networks contain units that, depending on the particular architecture of the network, resemble either the gain modulated neurons found in PRR or the partially shifting (and gain modulated) cells found in area 5.

Methodological issues

For our population analysis (Fig. 6), invariability was calculated using 200 ms long time bins centered on consecutive 100 ms intervals of the task. This analysis showed that in both area 5 and PRR there is a dominant spatial representation that exists soon after the cue is presented and continues to dominate until at least the early part of the movement. Although it is conceivable that coordinate transformations occurred soon after cue presentation and over a shorter time interval than was examined here, this should have resulted in both areas appearing dominantly hand-centered (the presumed end stage of the transformation) from a point soon after the cue was presented and throughout the rest of the task, which was not the case in either area 5 or PRR. Thus, we believe that our choice of time bins did not adversely affect our interpretation of this analysis, and that the spatial representations in both area 5 and PPR are in fact invariant with respect to time, at least in this task.

For our single cell analysis, we initially included all of the cells from each area. When all cells were tested, we found that the majority of neurons in both areas did not switch reference frames between epochs, though the percentage of cells that did appear to switch was significant, particularly in area 5. However, this result was related to the inclusion of neurons which, statistically speaking, did not have a single, best-fitting combination of reach variables in one or more of the behavioral epochs. As described in "Results", when such cells were excluded from the analysis, only a very small percentage of cells in each area showed evidence of a reference frame switch with time. However, the imposition of this criterion meant that a relatively large number of cells were excluded from this analysis. While the exclusion of such cells is justified, we acknowledge that it may have led to an underestimation of the number of individual cells that switch reference frames, though our population analysis indicates these cells likely to do not exist in sufficiently large numbers to affect the representation at the population level.

Acknowledgments The authors wish to thank Betty Gillikin, Kelsie Pejsa, Lea Martel and Viktor Shcherbatyuk for technical assistance, Janet Baer and Janna Wynne for veterinary care and Cierina Marks and Tessa Yao for administrative assistance. This work was supported by the J. G. Boswell Foundation, the Sloan-Swartz Center for Theoretical Neurobiology, the National Eye Institute (NEI), the Defense Advanced Research Projects Agency (DARPA), and the Office of Naval Research (ONR).

References

Batista AP, Buneo CA, Snyder LH, Andersen RA (1999) Reach plans in eye-centered coordinates. Science 285:257–260

Battaglia-Mayer A, Ferraina S, Mitsuda T, Marconi B, Genovesio A, Onorati P, Lacquaniti F, Caminiti R (2000) Early coding of reaching in the parietooccipital cortex. J Neurophysiol 83:2374–2391

Battaglia-Mayer A, Ferraina S, Genovesio A, Marconi B, Squatrito S, Molinari M, Lacquaniti F, Caminiti R (2001) Eye-hand coordination during reaching. II. An analysis of the relationships between visuomanual signals in parietal cortex and parieto-frontal association projections. Cereb Cortex 11:528–544

Buneo CA, Andersen RA (2006) The posterior parietal cortex: sensorimotor interface for the planning and online control of visually guided movements. Neuropsychologia 44:2594–2606

Buneo CA, Jarvis MR, Batista AP, Andersen RA (2002) Direct visuomotor transformations for reaching. Nature 416:632–636

Buneo CA, Jarvis MR, Batista AP, Andersen RA (2003) Properties of spike train spectra in two parietal reach areas. Exp Brain Res 153:134–139

Burnod Y, Baraduc P, Battaglia-Mayer A, Guigon E, Koechlin E, Ferraina S, Lacquaniti F, Caminiti R (1999) Parieto-frontal coding of reaching: an integrated framework. Exp Brain Res 129:325–346

Caminiti R, Ferraina S, Mayer AB (1998) Visuomotor transformations: early cortical mechanisms of reaching. Curr Opin Neurobiol 8:753–761

Crawford JD, Medendorp WP, Marotta JJ (2004) Spatial transformations for eye-hand coordination. J Neurophysiol 92:10–19

Deneve S, Latham PE, Pouget A (2001) Efficient computation and cue integration with noisy population codes. Nat Neurosci 4:826–831

Efron B, Tibshirani RJ (1993) An introduction to the bootstrap. Chapman and Hall, London

Flanders M, Helms-Tillery SI, Soechting JF (1992) Early stages in a sensorimotor transformation. Behav Brain Sci 15:309–362

Flanders M, Hondzinski JM, Soechting JF, Jackson JC (2003) Using arm configuration to learn the effects of gyroscopes and other devices. J Neurophysiol 89:450–459

Henriques DY, Klier EM, Smith MA, Lowy D, Crawford JD (1998) Gaze-centered remapping of remembered visual space in an open-loop pointing task. J Neurosci 18:1583–1594

Kalaska JF, Crammond DJ (1995) Deciding not to go—neuronal correlates of response selection in a go/nogo task in primate premotor and parietal cortex. Cereb Cortex 5:410–428

McIntyre J, Stratta F, Lacquaniti F (1998) Short-term memory for reaching to visual targets: psychophysical evidence for body-centered reference frames. The J Neurosci 18:8423–8435

Messier J, Kalaska JF (2000) Covariation of primate dorsal premotor cell activity with direction and amplitude during a memorized-delay reaching task. J Neurophysiol 84:152–165

Russo GS, Backus DA, Ye SP, Crutcher MD (2002) Neural activity in monkey dorsal and ventral cingulate motor areas: comparison with the supplementary motor area. J Neurophysiol 88:2612–2629

Salinas E, Abbott LF (1995) Transfer of coded information from sensory to motor networks. J Neurosci 15:6461–6474

Shen LM, Alexander GE (1997) Neural correlates of a spatial sensory-to-motor transformation in primary motor cortex. J Neurophysiol 77:1171–1194

Smith MA, Crawford JD (2001) Self-organizing task modules and explicit coordinate systems in a neural network model for 3-D saccades. J Comput Neurosci 10:127–150

Snyder LH, Batista AP, Andersen RA (1997) Coding of intention in the posterior parietal cortex. Nature 386:167–170

Snyder LH, Batista AP, Andersen RA (2000) Intention-related activity in the posterior parietal cortex: a review. Vision Res 40:1433–1441

Wise SP, Boussaoud D, Johnson PB, Caminiti R (1997) Premotor and parietal cortex: corticocortical connectivity and combinatorial computations. Annu Rev Neurosci 20:25–42

Xing J, Andersen RA (2000) Models of the posterior parietal cortex which perform multimodal integration and represent space in several coordinate frames. J Cogn Neurosci 12:601–614

Zar JH (1996) Biostatistical Analysis. Prentice Hall, NJ

Zipser D, Andersen RA (1988) A back-propagation programmed network that simulates response properties of a subset of posterior parietal neurons. Nature 331:679–684